Available online at www.sciencedirect.com

ScienceDirect

Procedia Structural Integrity 49 (2023) 3–9

Structural Integrity Procedia

www.elsevier.com/locate/procedia

Medical Devices: Materials, Mechanics and Manufacturing

2nd International Conference on Medical Devices: Materials, Mechanics and Manufacturing (ICMD3M 2023)

Computational fluid dynamics analysis of the fluid environment of 3D printed tissue scaffolds within a perfusion bioreactor: the effect of pore shape

Bin Zhang[a]*

[a] *Department of Mechanical and Aerospace, Brunel University London, UK*

Abstract

Mass transport properties within 3D scaffold are essential for tissue regeneration; for example, various fluid environmental cues influence mesenchymal stem cells (MSCs) differentiation. 3D printing has been emerging as a new technology for scaffold fabrication by controlling the scaffold pore geometry to influence cell growth environment. Direct ink writing, one of the popular 3D printing methods, has the advantages of controlling the structure design and material selections. In this study, woodpile lattice tissue scaffold was fabricated using DIW method. The flow field within lattice scaffolds in a perfusion system was investigated with angles from 90° to 15° using the computational fluid dynamics (CFD) method. The results indicate that the maximum fluid velocity magnitude and fluid shear stress within the unit pore geometries of lattice structures increased as the angle decreased from 90° to 15°. The application of CFD techniques allowed a detailed prediction of velocity and fluid shear stress mapping within 3D printed scaffolds which is crucial to determine the optimal environment for cell and nutrient transport.

Keywords: 3D printing; tissue scaffolds; pore shape; computational fluid dynamics.

* Corresponding author. Tel.: +44 1895 268573
E-mail address: bin.zhang@brunel.ac.uk

10.1016/j.prostr.2023.10.002

1. Introduction

Three-dimensional (3D) printing has been emerging as a new technology for scaffold fabrication to overcome problems such as uncontrollable or undesirable microstructure of traditional methods, which could limit tissue formation (Zhang, Huang and Narayan, 2020). Direct ink writing (DIW), one of the popular 3D printing methods, has advantages of customizing the structure design and material selections. re-prepared biomaterial ink can be extruded via a computer-controlled nozzle to build a 3D construct layer by layer at room temperature. It is attractive for biomanufacturing due to the heat-free approach and avoid the risk of material degradation, which can open up a number of clinical possibilities (Park, Lee and Kim, 2011; Zhang et al., 2020; Zhang et al., 2022).

Bone scaffolds serve as supporting structures for cell proliferation, migration, and differentiation. Viewed as porous structures, the scaffolds pores should be well connected to allow the flow of culture medium with cells, nutrients, and oxygen within the scaffold. Appropriate mechanical stimuli should be able to be transmitted to the scaffold so that cells can follow specific differentiation pathways (Loh and Choong, 2013). Fluid flow can be applied to scaffolds and transmit mechanical stimuli to cells attached to the scaffold surface, which stimulates tissue differentiation by fluid shear stress (Meyer et al., 2006). Quite a few studies used perfusion fluid flow bioreactors to investigate the relationship between appropriate shear stress and cell differentiation. One of the advantages is that the perfusion fluid flow system can stimulate cell differentiation by mimicking the interstitial fluid flow of extravascular fluid through the extracellular matrix in the human body (Martin, Wendt and Heberer, 2004). When a perfusion fluid is applied, the fluid flows through the interconnected pores generating the fluid shear stress at the scaffold surface.

There are some studies investigating the influence of scaffold pore distribution and pore geometry, i.e., pore size, porosity on fluid shear stress. Boschetti et al. (2004) showed that the pore size is a variable strongly influencing the predicted level of shear stress, whereas the porosity is a variable strongly affecting the statistical distribution of the shear stresses, but not their magnitude. Olivares et al. (2009) indicated that the distribution of shear stress induced by fluid perfusion is very dependent on pore distribution within the scaffold. Melchels et al. (2011) simulated the fluid shear stress within uniform gyroid scaffold in perfusion fluid and compared the simulation results with in vitro experiments. The results revealed that there was the highest cell density in the region of the scaffold where the wall shear stress of the fluid flow was the highest (3.8×10^{-3} Pa). Based on the above studies, it is evident that the distribution of fluid field within scaffold can affect the cell distribution, and MSCs show the potential to differentiate various cells with influencing by fluid shear stress. However, the distribution of fluid shear stress on scaffolds that lead to functional tissue requires in-depth understanding. The Finite element method is one of the computational techniques to study the mechanical stimuli distribution on the scaffold. This study aims to analyse the influence of scaffold pore shape on the response of the interstitial fluid velocity and surface shear stress within the scaffold's pores at the initial stage of a perfusion bioreactor cell culture.

2. Material and method

2.1. Design of CAD scaffold structures

To mimic the fluid environment in a perfusion bioreactor, CAD scaffolds were designed as layered cylinders with a diameter of 9 mm using Solidworks software (SolidWorks, 2016, Santa Monica, CA, USA). Lattice scaffolds with angles of 15°, 30°, 45°, 60°, and 90° were designed. As shown in Fig. 1 (A), the pore size (*dxy*) is defined as the inter-filament spacing, which is set as 400 μm, and the filament diameter (*d*) is 600 μm. The layer overlap between layers (*f*) is 180 μm. All lattice scaffolds formed with six layers.

2.2. Computational fluid dynamics (CFD) model

The CAD scaffold models were imported into Fluent 17.0 (ANSYS, Inc.) for CFD simulations. The lattice scaffold was placed in the middle of a 50 mm long tube. The diameter of the tube is able to completely enclose the cylindrical scaffold. The distance between the inlet and the scaffold is 25 mm, which is sufficiently long to create a fully developed laminar flow condition. The mesh is created with tetrahedral elements using 'curvature' setting in Fluent 17.0 (ANSYS, Inc.); the curvature ratio is set as the default value 1.2. This meshing method can provide a smooth

transition from the surroundings of the scaffold to the internal pores. The minimum element size is 16 μm inside the pores and the maximum element size is 1 mm far away from the scaffold. The total number of tetrahedral elements is 24 million, which is determined by a mesh sensitivity study.

2.3. Ink formulation and 3D printing

Suitable inks were prepared considering the properties of the composite ink are crucial factors which affect the continuity and stability of the direct ink writing 3D printing fabricating process. PCL (Mw=80,000 g · mol^{-1}) and PEO (Mw=60,000 g · mol^{-1}) were purchased from Sigma-Aldrich (USA). Trisolvent mixture – dichloromethane (DCM), 2-butoxyethanol (2-Bu), and dibutyl phthalate (DBP) were purchased from VWR (USA). The mixed solvent was used to dissolve PCL and PEO copolymer (weight ratio as 1:1) were prepared by gentle magnetic stirring at 200 rpm for 3 hours at the 25°C temperature. Hydroxyapatite (HAp) nanoparticles (SkySpring nanomaterials, Inc) with particle size less than 40 nm was added in the PCL/PEO solution with respect to the required weight percentage from 55% to 85% and stirring for 8 h for obtaining the homogenous solution.

The 3D printing fabrication process is carried out at room temperature (25°C), and the formulated ink was loaded into a 3 ml syringe is used to carry out the extrusion. The R3bel 3D bioprinter (SE3D, Santa Clara, CA, United States), piston extrusion bioprinting, was applied to fabricate the scaffolds. Glass slide is put on the workbench before extrusion, enabling a smooth and flat surface. These scaffolds can be taken off from glass slides after drying.

3. Result and discussion

3.1. 3D printing tissue scaffold

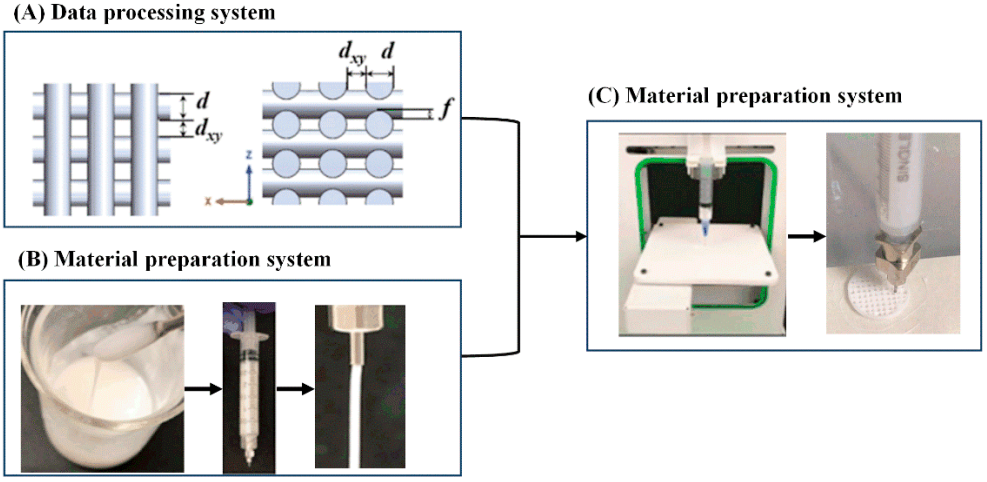

Fig. 1. Schematic of printing a PCL/PEO/HAp scaffold using the direct ink writing technique.

Polycaprolactone (PCL) has been approved by the U.S. Food and Drug Administration and successfully used as tissue engineering scaffolds. However, PCL is hydrophobic in nature, and the degradation rate is relatively slow, which limits its applications when a faster degradation is desirable. Blending PCL with hydrophilic polymers, such as PEO, facilitates the modulation of its surface wettability and degradation profile, which has been reported by various researchers (Lyons, Blackie and Higginbotham, 2008; Remya et al., 2018). HAp is one of bioactive ceramics for bone tissue engineering mainly owing to its primary constitution of bone minerals. The application of HAp particles has the potential to enhance osteoinductivity and osseointegration, which can improve the biomechanical strength due to the formation of the strong chemical bond with bone (Murugan and Ramakrishna, 2005). The combination of polymer and ceramic materials offers unique properties and presents great prospects in regenerative medicine.

Fig. 1 shows the flow chart of the scaffold printing process. There are three subsystems in the 3D printing fabrication system, which are the data processing system, material preparation system, and computer control system. The continuity and consistency of the co-polymer inks extruding process are of great importance during the 3D

printing process. The fabrication process details were reported in our previous study (Zhang et al., 2022), and the extruding process can be affected by the inks, fabrication structure, and configuration of fabrication parameters.

3.2. Mesh sensitivity test for CFD modelling

A mesh sensitivity test is conducted to determine the appropriate mesh size for CFD simulations. First, the flow velocity and fluid shear stress are compared between five gradually reducing mesh sizes for the pores of a 90° lattice scaffold in CFD modelling. In Fig. 2 (A), the fluid velocities are extracted from line 1 on layer 3 in the scaffold. The average velocity only changes by about 0.5% by reducing the minimum element size from 16 μm to 4 μm; however, a minimum element size of 4 μm requires almost twice as much computational time as that of a minimum element size of 16 μm needs. The maximum shear stress on the scaffold only changes less than 0.2% when reducing the minimum element size from 16 μm to 4 μm. Therefore, a minimum element size of 16 μm is chosen for the pores in CFD modelling.

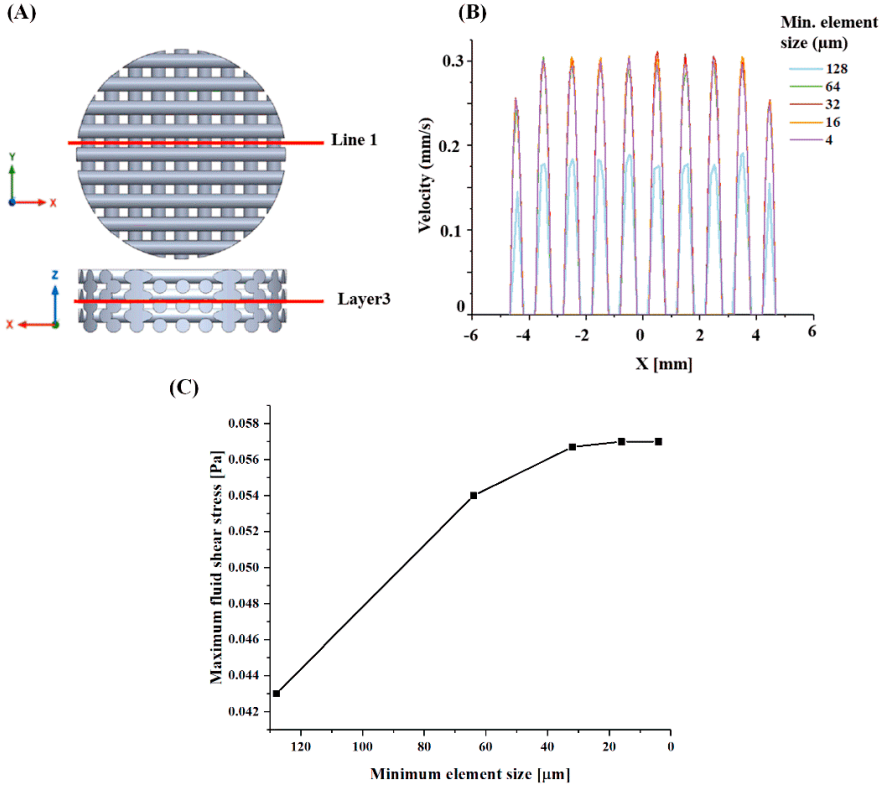

Fig. 2: (A) 90° lattice scaffold in CFD modelling. (B) Plots of flow velocities inside the pores of a 90° lattice scaffold for different element sizes in CFD modelling. The velocities are extracted from line 1 on layer 3. The zero-velocity regions along the *X*-direction correspond to solid filaments, which have no fluid flow going through. (C) Plot of maximum shear stress on the scaffold vs. minimum element sizes for the pores of a 90° lattice scaffold in CFD modelling.

3.3. Local fluid dynamics in pores

For those lattice structures, the higher fluid velocity was observed in the middle of the pores in those lattice scaffolds. Fig. 3 (A, B) shows the detailed view of unit pore geometry. The fluid velocity in the middle of the pore gradually increases with the filament angle changing from 90° to 15°. The highest fluid velocity magnitude of 3.73 mm/s (Table 1) was found in the middle of 15° lattice scaffold, which is approximately seven times of the inlet velocity (0.5 mm/s). For a more detailed comparison of fluid velocity within the scaffolds, the histogram of fluid velocity in a transversal section of the scaffold was plotted, as shown in Fig. 4 (A). Although most of the fluid velocity values were

in the lower end, i.e., 0-0.5 mm/s, there was a large variation between the highest fluid velocity and lowest velocity for those lattice scaffolds. Especially for 15° lattice scaffold, there is about 45% fluid velocity locates in the range of 0–0.5 mm/s, while its highest fluid velocity is greater than 3.5 mm/s.

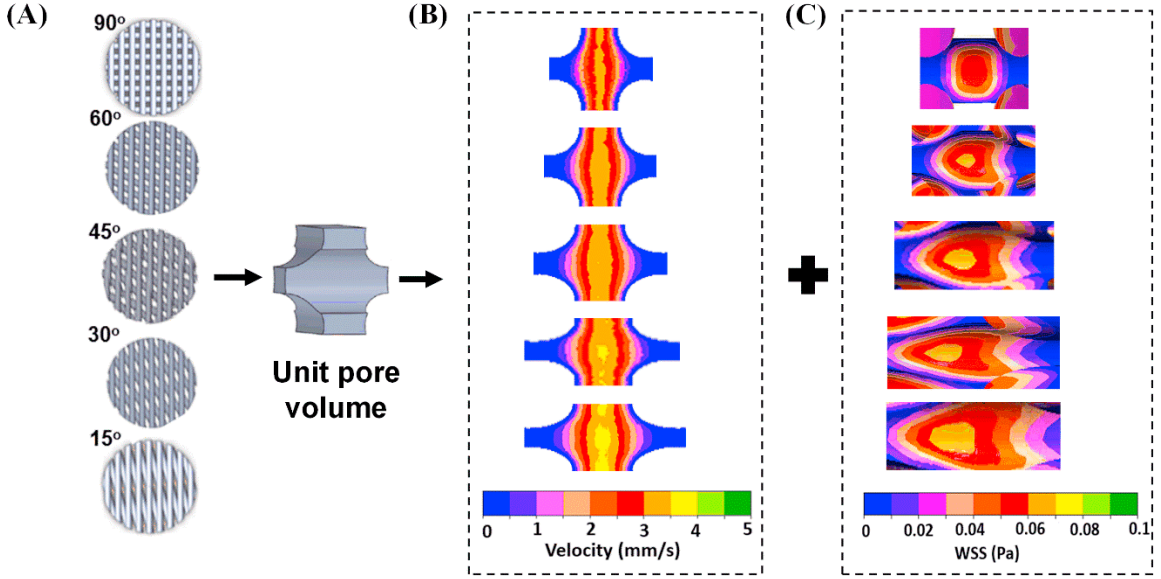

Fig. 3. CAD model of lattice scaffold (A). Fluid velocity magnitude distribution (B) and WSS (C) within the unit pore geometries of the 90°, 60°, 45°, 30°, and 15° lattice structure.

Table 1. 3D lattice scaffold unit pore volume and max. fluid velocity and WSS.

Scaffold type	Unit pore volume (mm^3)	Max. fluid velocity (mm/s)	Max. WSS (Pa)
90° lattice	0.39	3.22	0.057
60° lattice	1.84	3.35	0.062
45° lattice	2.28	3.41	0.065
30° lattice	3.2	3.47	0.066
15° lattice	6.16	3.73	0.068

The fluid shear stress is directly proportional to the velocity gradient. The fluid shear stress distribution in scaffolds. The highest fluid shear stress locates in the middle area of unit pore geometries (Fig. 2 (C)). The fluid shear stress increased with the lattice scaffold angles decreasing from 90° to 15°. The maximum fluid shear stress was similar among those scaffolds. For detailed comparison of fluid shear stress distributions within the scaffolds, the histogram of fluid shear stress in a transversal section of the centre of the scaffold was plotted, as shown in Fig. 4 (B). The trend is similar to the fluid velocity, and the maximum fluid shear stress (0.068 Pa) also locates in the middle section of 15° lattice scaffolds. There is a large frequency locates in the lower end of shear stress, i.e., 0 to 0.01 Pa, for all those lattice scaffolds. However, the fluid shear stress frequency distribution for those lattice scaffolds also has a variation between the highest fluid shear stress and lowest shear stress (0.01 Pa).

It is worth mentioning that uncoupled fluid-structure were assumed for the scaffold. This approximation does not consider the influence of scaffold deformation generated by the fluid flow, and the scaffold was assumed as rigid and impermeable. Since the maximum fluid shear stress on the scaffolds was less than 0.068 Pa (Table 1), it is assumed that the filament deformation caused by solid-fluid interaction can be neglected.

Scaffolds are mechanical supporting structures that transmit mechanical stimulus to the cell scale to stimulate tissue synthesis and control the phenotype of the formed tissue. Although the influence of scaffold structure on fluid velocities and shear stresses have been reported in the literature review, it is controversial about the range of shear stresses for MSCs response in the literature (Kim et al., 2011; Yu et al., 2014; Zhao, Chella and Ma, 2007). The discrepancy between those studies can be attributed to the use of different architecture, dimensions, scaffold material, and experimental conditions. It is difficult to measure the local mechanical stimuli sensed by the cells at a pore level in the experiment. Thus, the predictions of fluid shear stress and fluid path on regular architecture through

computational fluid dynamic (CFD) offer a tool to determine the design parameters (Boschetti et al., 2006).

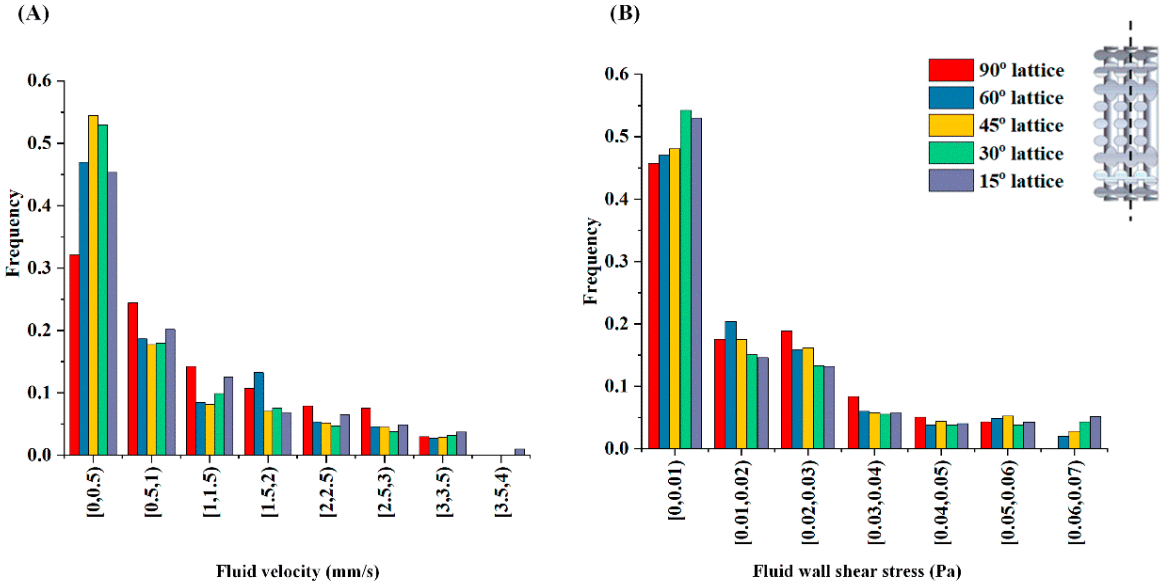

Fig. 4. Histogram of fluid velocity under perfusion fluid flow (A) and fluid wall shear stress under perfusion fluid flow (B). Only nodes in a transversal section in the centre of the scaffold were plotted.

Kim et al. (2011) indicated that the interstitial flow produces lower shear stress than blood flow, and mesenchymal stem cells (MSCs) may receive interstitial shear stress of the order of 0.01 Pa to 0.1 Pa under physiological conditions. Studies focused on the MSCs induces osteogenesis in 3D culture have employed fluid shear stress in the range of 0.01–0.05 Pa (Brindley et al., 2011; Wittkowske et al., 2016). In this study, 3D scaffold pore geometry has been investigated by changing the filament stack position. Thus the fluid shear stress and fluid velocity distribution patterns are different. Most of the frequency of fluid shear stress of those scaffolds locate in the range of 0–0.05 Pa.

Also, some CFD studies (Byrne et al., 2007; Geris et al., 2004; Liu and Niebur, 2008; Olivares et al., 2009) applied the mechano-regulation theory (Prendergast, Huiskes and Søballe, 1997) to predict tissue differentiation in the application of bone tissue. In this theory, the mechanical stimuli were not only raised from the compressive strain but also the fluid shear stress generated from the liquid phase. The thresholds of mechanical stimuli value S is in the range of $0.001 \leq S \leq 1$, $1 \leq S \leq 3$, and $3 \leq S \leq 6$, corresponding to formation of bone, cartilage, and fibrous tissue, respectively; while resorption and necrosis occur when $S<0.001$ and $S \geq 6$ respectively.

The complexity of the biological process that occurs on cell dynamics was not included in the simulations of this study. The primary biological assumption is that cells can penetrate through the entire volume until all the available space is occupied. Therefore, according to mechano-regulation theory, the simulation results suggest that the different distribution of fluid shear stress can induce different cell differentiation patterns on the scaffold surfaces. Also, the ability to control fluid velocity and fluid shear stress distributions on scaffolds have opened the door to multiple tissue and tissue interface regeneration.

4. Conclusion

The woodpile lattice scaffold with newly formulated biocomposite PCL/PEO/HAp inks was fabricated using direct ink writing 3D printing. The work systematically with CFD modelling to investigate the magnitude and statistical distribution of fluid velocity and shear stress on the scaffolds with different pore shapes (i.e., lattice structure with angles from 15-90°). The results demonstrate that velocity and wall shear stress distribution varied in different filament angles of 3D printing scaffolds, which could influence the initial conditions for cell attachment on scaffolds under fluid flow. Different fluid flow distribution was found within the scaffolds, suggesting that cells would be exposed to different stimulations, which could guide the development of scaffolds for multi-phase tissue.

Acknowledgements

Dean Prize of University College London engineering department scholarship is gratefully acknowledged.

References

Boschetti, F., Pennati, G., Gervaso, F., Peretti, G.M., Dubini, G., 2004. Biomechanical properties of human articular cartilage under compressive loads. Biorheology 41, 159-166.

Boschetti, F., Raimondi, M.T., Migliavacca, F., Dubini, G., 2006. Prediction of the micro-fluid dynamic environment imposed to three-dimensional engineered cell systems in bioreactors. Journal of biomechanics 39, 418-425.

Brindley, D., Moorthy, K., Lee, J.-H., Mason, C., Kim, H.-W., Wall, I., 2011. Bioprocess forces and their impact on cell behavior: implications for bone regeneration therapy. Journal of tissue engineering 2011.

Byrne, D.P., Lacroix, D., Planell, J.A., Kelly, D.J., Prendergast, P.J., 2007. Simulation of tissue differentiation in a scaffold as a function of porosity, Young's modulus and dissolution rate: application of mechanobiological models in tissue engineering. Biomaterials 28, 5544-5554.

Geris, L., Andreykiv, A., Van Oosterwyck, H., Vander Sloten, J., Van Keulen, F., Duyck, J., Naert, I., 2004. Numerical simulation of tissue differentiation around loaded titanium implants in a bone chamber. Journal of biomechanics 37, 763-769.

Kim, D.H., Heo, S.-J., Kim, S.-H., Shin, J.W., Park, S.H., Shin, J.-W., 2011. Shear stress magnitude is critical in regulating the differentiation of mesenchymal stem cells even with endothelial growth medium. Biotechnology letters 33, 2351-2359.

Liu, X., Niebur, G.L., 2008. Bone ingrowth into a porous coated implant predicted by a mechano-regulatory tissue differentiation algorithm. Biomechanics and Modeling in Mechanobiology 7, 335.

Loh, Q.L., Choong, C., 2013. Three-dimensional scaffolds for tissue engineering applications: role of porosity and pore size. Tissue Engineering Part B: Reviews 19, 485-502.

Lyons, J.G., Blackie, P., Higginbotham, C.L., 2008. The significance of variation in extrusion speeds and temperatures on a PEO/PCL blend based matrix for oral drug delivery. International journal of pharmaceutics 351, 201-208.

Martin, I., Wendt, D., Heberer, M., 2004. The role of bioreactors in tissue engineering. TRENDS in Biotechnology 22, 80-86.

Melchels, F.P., Tonnarelli, B., Olivares, A.L., Martin, I., Lacroix, D., Feijen, J., Wendt, D.J., Grijpma, D.W., 2011. The influence of the scaffold design on the distribution of adhering cells after perfusion cell seeding. Biomaterials 32, 2878-2884.

Meyer, U., Büchter, A., Nazer, N., Wiesmann, H., 2006. Design and performance of a bioreactor system for mechanically promoted three-dimensional tissue engineering. British Journal of Oral and Maxillofacial Surgery 44, 134-140.

Murugan, R., Ramakrishna, S., 2005. Development of nanocomposites for bone grafting. Composites Science and Technology 65, 2385-2406.

Olivares, A.L., Marsal, È., Planell, J.A., Lacroix, D., 2009. Finite element study of scaffold architecture design and culture conditions for tissue engineering. Biomaterials 30, 6142-6149.

Park, S.A., Lee, S.H., Kim, W.D., 2011. Fabrication of porous polycaprolactone/hydroxyapatite (PCL/HA) blend scaffolds using a 3D plotting system for bone tissue engineering. Bioprocess and biosystems engineering 34, 505-513.

Prendergast, P., Huiskes, R., Søballe, K., 1997. Biophysical stimuli on cells during tissue differentiation at implant interfaces. Journal of biomechanics 30, 539-548.

Remya, K., Chandran, S., Mani, S., John, A., Ramesh, P., 2018. Hybrid Polycaprolactone/Polyethylene oxide scaffolds with tunable fiber surface morphology, improved hydrophilicity and biodegradability for bone tissue engineering applications. Journal of Biomaterials Science, Polymer Edition 29, 1444-1462.

Wittkowske, C., Reilly, G.C., Lacroix, D., Perrault, C.M., 2016. In Vitro Bone Cell Models: Impact of Fluid Shear Stress on Bone Formation. Frontiers in bioengineering and biotechnology 4.

Yu, W., Qu, H., Hu, G., Zhang, Q., Song, K., Guan, H., Liu, T., Qin, J., 2014. A microfluidic-based multi-shear device for investigating the effects of low fluid-induced stresses on osteoblasts. PloS one 9, e89966.

Zhang, B., Cristescu, R., Chrisey, D.B., Narayan, R.J., 2020. Solvent-based Extrusion 3D Printing for the Fabrication of Tissue Engineering Scaffolds. International Journal of Bioprinting 6.

Zhang, B., Huang, J., Narayan, R., 2020. Gradient scaffolds for osteochondral tissue engineering and regeneration. Journal of Materials Chemistry B.

Zhang, B., Nguyen, A.K., Narayan, R.J., Huang, J., 2022. Direct ink writing of vancomycin-loaded polycaprolactone/polyethylene oxide/hydroxyapatite 3D scaffolds. Journal of the American Ceramic Society 105, 1821-1840.

Zhao, F., Chella, R., Ma, T., 2007. Effects of shear stress on 3-D human mesenchymal stem cell construct development in a perfusion bioreactor system: Experiments and hydrodynamic modeling. Biotechnology and bioengineering 96, 584-595.